

Published in final edited form as:

Biochemistry. 2011 March 22; 50(11): 1910–1916. doi:10.1021/bi1017182.

The Reaction of the Molybdenum- and Copper-Containing Carbon Monoxide Dehydrogenase from *Oligotropha carboxydovorans* with Quinones[†]

Jarett Wilcoxon, Bo Zhang, and Russ Hille*

Department of Biochemistry, University of California, Riverside, CA 92521

Abstract

Carbon monoxide dehydrogenase (CODH) from *Oligotropha carboxydovorans* catalyzes the oxidation of carbon monoxide to carbon dioxide, providing the organism both a carbon source and energy for growth. In the oxidative half of the catalytic cycle, electrons gained from CO are ultimately passed to the electron transport chain of the Gram-negative organism, but the proximal acceptor of reducing equivalents from the enzyme has not been established. Here we investigate the reaction of reduced enzyme with various quinones, and find them to be catalytically competent. Benzoquinone has a k_{ox} of 125.1 s^{-1} and K_d of $48 \text{ }\mu\text{M}$; ubiquinone-1 has a k_{ox}/K_d value of $2.88 \times 10^5 \text{ M}^{-1}\text{s}^{-1}$; 1,4-naphthoquinone has a k_{ox} of 38 s^{-1} and K_d of $140 \text{ }\mu\text{M}$; and 1,2-naphthoquinone-4-sulfonic acid a k_{ox}/K_d of $1.31 \times 10^5 \text{ M}^{-1}\text{s}^{-1}$. An extensive effort to identify a cytochrome that was reducible by CO/CODH was unsuccessful. Steady-state studies with benzoquinone indicate that the rate-limiting step is in the reductive half of the reaction (that is, the reaction of oxidized enzyme with CO). On the basis of the inhibition of CODH by diphenyliodonium chloride we conclude that quinone substrates interact with CODH at the enzyme's flavin site. Our results strongly suggest that CODH donates reducing equivalents directly to the quinone pool without using a cytochrome as an intermediary.

Molybdenum-containing enzymes are very broadly distributed in biology, and members of the xanthine oxidoreductase (XOR) family comprise a large and important group of these enzymes. Family members generally catalyze the oxidative hydroxylation of aromatic heterocycles and aldehydes, and the reducing equivalents generated in this process pass from the molybdenum center, where catalysis takes place, through two [2Fe-2S] clusters and (in most cases) on to an FAD where the electrons are passed on to an oxidizing substrate such as NAD^+ or O_2 (1).

Carbon monoxide dehydrogenase (CODH) from aerobic, chemolithotrophic organisms such as *Oligotropha carboxydovorans* and *Hydrogenophaga pseudoflava* is clearly a member of the xanthine oxidase family based on its overall amino acid sequence and three-dimensional structure (2-8). The functional enzyme is a $(\alpha\beta\gamma)_2$ hexamer that consists of a small 17.8 kDa subunit (CoxS) containing two [2Fe-2S] clusters, a medium 30.2 kDa subunit (CoxM) containing an FAD cofactor, and a large 88.7 kDa subunit (CoxL) that possesses the molybdenum center. CODH is encoded by the mega plasmid pHCG3 in the CoxMSL cluster (9,10). The overall protein fold notwithstanding, two aspects make CODH unique in the

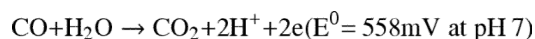
[†]This work was supported by the National Institute of Health Grant GM 075036 (to R.H.).

*Correspondence addressed. Department of Biochemistry, 1462 Boyce Hall, University of California, Riverside, Riverside, CA 92521
Tel: 951-827-6354 Fax: 951-827-2364 Russ.hille@ucr.edu.

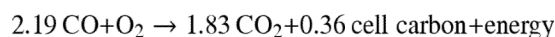
This material is available free of charge via the Internet at <http://pubs.acs.org>.

XOR family: first, the reaction itself is not strictly speaking a hydroxylation and does not involve the cleavage of a C-H bond; and second, the active site consists of a unique binuclear Mo-Cu center rather than a mononuclear molybdenum center such as is seen in all other family members. As shown in Figure 1, the active site is an $\text{LMo}^{\text{VI}}\text{O}_2\text{-(}\mu\text{S)-Cu}^{\text{I}}\text{-SCys}$ cluster, where L represents the pyranopterin cofactor found in all molybdenum (and tungsten) containing enzymes other than nitrogenase (4,5,11). The Mo/Cu-containing CODH from *O. carboxydovorans* and *Hydrogenophaga pseudoflava* is structurally and mechanistically distinct from the Fe/Ni-containing CODH of the acetogen *Moorella thermoacetica* or the methanogen *Methanosarcina barkerii* (12).

In the reaction carried out by CODH, CO is oxidized to CO_2 , yielding two reducing equivalents according to the following stoichiometry:



The reducing equivalents thus obtained by the enzyme are passed to the electron transport chain to provide energy for cell growth. A portion of the CO_2 generated as a product of the reaction is fixed non-photosynthetically by the pentose phosphate cycle (13,14) with an overall stoichiometry of:



The overall reaction is of profound environmental importance, since aerobic bacteria such as *O. carboxydovorans* clear an estimated 2×10^8 metric tons of CO from the atmosphere annually (15).

It has been suggested that reducing equivalents are removed from CODH by either cyt b_{561} or the quinone pool, although no definitive evidence has been provided in support of either (13,16). In the present study we have investigated the kinetics involved with the oxidative half-reaction of the enzyme with various quinones, and find that they serve very effectively as oxidizing substrates for CODH, reacting with reduced enzyme with rate constants large enough to support catalysis. By contrast, cytochrome b_{561} is found not to readily accept reducing equivalents from reduced CODH, and we are unable to identify any other cytochrome from *O. carboxydovorans* capable of doing so. We conclude that quinones are the likely physiological oxidant of CODH.

MATERIALS AND METHODS

Materials

Carbon monoxide gas was obtained from Air, Inc. at a purity of 99.5%. 1,4-benzoquinone, 1,2-naphthoquinone-4-sulfonic acid, 1,4-naphthoquinone, and ubiquinone-1 were purchased from Sigma-Aldrich. Isotopically enriched D_2O was obtained from Cambridge Isotope Lab, Inc. All other chemicals and reagents were obtained at the highest quality and purity commercially available and used without additional purification.

Bacterial cultivation and enzyme purification

O. carboxydovorans (ATCC 49405) cells were grown at 30°C , pH 7 in a 20 L fermentor (BioFlo 415, New Brunswick) containing Minimal Medium and CO as the carbon source (introduced as a mixture of 50% CO and 50% air). Cells were harvested in late log phase ($\text{OD}_{436} > 5$), washed in 50 mM HEPES (pH 7.2) and stored at -80°C until needed (17).

CODH was purified according to the procedure described by Zhang *et al.* (18), using a combination of Q-Sepharose and Sephacryl S-300 FPLC chromatography.

Cytochrome b_{561} was purified from *O. carboxydovorans* grown as described above. 100 g of thawed cells were resuspended in 50 mM HEPES (pH 7.2) containing 1 mM EDTA, 5 mg DNase, 0.2 mM PMSF and broken open by French press (FA-078A, Thermo Electron Co.). Cell debris were separated by ultra centrifugation at $100k \times g$ for 2 h. Cell membranes were solubilized in 50 mM HEPES (pH 7.2) containing 1 mM EDTA, 0.2 mM PMSF and 10% v/v Triton X-100. The non-solubilized membranes were separated by ultra centrifugation at $100k \times g$ for 2 h. The soluble fraction was loaded onto a CM anion exchange column (11 cm \times 1.5 cm) using an ÄKTA FPLC apparatus (GE Healthcare) at 4°C; the column was pre-equilibrated with 50 mM HEPES (pH 7.2) containing 0.1 mM EDTA and 0.2% Triton X-100. Elution was carried out over 10 column volumes in a linear gradient from 0 mM to 500 mM NaCl. Fractions containing cytochrome b_{561} were pooled and concentrated using an Amicon concentrator equipped with a 10 kDa cutoff filter. The identity of cytochrome b_{561} was verified by UV-vis spectroscopy with an absorbance peak at 415 nm in the oxidized cytochrome and 425 nm, 530 nm, and 561 nm in the reduced cytochrome (Supplementary Material, Figure 1). Approximately 20-50 μ g of cytochrome b_{561} was obtained from 100 g of cells. Fractions containing other cytochromes were also saved and examined for activity with CODH.

Protein determination and activity assay

Enzyme quantity was determined by the absorbance at 450 nm ($\epsilon_{450}=70 \text{ mM}^{-1}\text{cm}^{-1}$) and 550 nm and purity assessed by the ratios of absorbance at 280 nm, 420 nm, 450 nm and 550 nm: the purified enzyme had absorbance ratios of $A_{280}/A_{450} \sim 5.5$, $A_{450}/A_{550} \sim 2.9$ and $A_{450}/A_{420} > 1$ (18). Routine activity was determined by the CO-dependent reduction of methylene blue ($\epsilon_{615}=37.11 \text{ mM}^{-1}\text{cm}^{-1}$) at 30° C (3,18). A second assay utilized 1,4-benzoquinone as oxidizing substrate, following reduction of, *e.g.*, 50 μ M 1,4-benzoquinone at 246 nm using an HP 8452A UV-visible spectrophotometer. A serum-stoppered cuvette (Starna Cells, inc) containing 50 μ M 1,4-benzoquinone in 2 mL of 50 μ M HEPES, pH 7.2, was bubbled with 100% CO for 10-15 min in the dark, after which 10-20 μ L of 4 μ M anaerobic stock CODH solution was added by Hamilton syringe. The specific activity in units per mg was determined using an extinction change for 1,4-benzoquinone reduction, obtained from the extinction coefficient $\epsilon_{247}=20.6 \text{ mM}^{-1}\text{cm}^{-1}$ for the oxidized 1,4-benzoquinone (20), a reduced coefficient of $\epsilon_{247}=0.42 \text{ mM}^{-1}\text{cm}^{-1}$ determined by the equation: $\epsilon_{\text{red}}=(\text{Abs}_{\text{red}})(\epsilon_{\text{ox}})/(\text{Abs}_{\text{ox}})$ to give $\Delta\epsilon_{247}=20.2 \text{ mM}^{-1}\text{cm}^{-1}$ for 1,4-benzoquinone, with 1 unit of activity being defined as 1 μ mol CO oxidized per min at 30° C. The enzyme used in the present work exhibited a specific activity of approximately 8.

All enzyme preparations were reconstituted with sulfur and copper using a modification of the procedure of Resch *et al.* (19). *Ca.* 100 μ M CODH in 1.0 mL of 50 mM Tris-HCl, pH 8.2 was made anaerobic by alternately evacuating and flushing with O₂-scrubbed Ar gas over the course of an hour. Appropriate volumes of stock solutions of 10 mM methyl viologen and 100 mM Na₂S were added to give final concentrations of 0.1 mM and 2.0 mM, respectively, followed by the addition of a sufficient volume of a ~0.1 M dithionite stock solution to sustain the blue color of the reduced viologen. This was incubated at 20° C for 12-18 hr under an atmosphere of argon gas. The enzyme was then passed through a G-25 chromatography column equilibrated with anaerobic 50 mM Tris-HCl, pH 8.2 to remove excess Na₂S, dithionite and methyl viologen. A stock solution of 10 mM Cu(I)-thiourea was prepared by dissolving Cu(I)Cl, thiourea, and sodium ascorbate in a 1:3:1 (w/w) ratio in anaerobic water, and the enzyme solution then made 0.2 mM in Cu(I) using this solution and incubated 5-10 hr at 20° C. A final G-25 column, again equilibrated with anaerobic 50 mM Tris-HCl, pH 8.2, was used to remove excess Cu(I). The enzyme was assayed for activity as

described above, and the degree of functionality independently determined by comparing the extent of enzyme bleaching, as observed at 450 nm, by CO (which reduces only the fully functional enzyme) with that seen using dithionite (which reduces both functional and non-functional enzyme) enzyme (5). Our enzyme was approximately 40% active, comparable to the levels seen previously (19). Unless otherwise stated, enzyme concentrations are given as functional enzyme, corrected for the fraction of nonfunctional enzyme present.

Steady-state kinetics

Steady-state studies monitoring the reduction of ubiquinone-1 and 1,4-benzoquinone were performed by bubbling anaerobic solutions of each in 50 mM HEPES (pH 7.2) with CO for 15 min to give 1 mM CO (previous studies having shown that concentrations of CO above 100 μM were saturating in steady-state assays; 18). The concentration ranges used were 11 μM to 97 μM for ubiquinone-1 and 8.4 μM to 191 μM for 1,4-benzoquinone. The reaction was initiated by the addition of 10 μL of 2 μM CODH, and the reaction monitored by the spectral change at 275 nm or 246, respectively, over 300 s at 25°C. Activities were obtained from the initial slopes of each assay, calculated using $\epsilon_{278}=14.7 \text{ mM}^{-1}\text{cm}^{-1}$ for ubiquinone-1 (22) and $\Delta\epsilon_{247}=20.2 \text{ mM}^{-1}\text{cm}^{-1}$ for 1,4-benzoquinone.

A kinetic isotope study was performed under the same conditions as described above using 50 mM HEPES in D_2O (pD 7.6) with the addition of varying concentrations of ubiquinone-1 in D_2O . CODH in D_2O prepared by anaerobic buffer exchange G-25 column into 50 mM HEPES in D_2O (pD 7.6).

Rapid reaction kinetics

The oxidative half-reaction of CODH was monitored by stopped-flow spectroscopy (using an Applied Photophysics, Inc. SX-18MV. Standard reaction conditions were 50 mM HEPES, pH 7.2, 25°C. Enzyme at a concentration of $\sim 10 \mu\text{M}$ before mixing was placed in a glass tonometer equipped with a sidearm cuvette and made anaerobic by repeated evacuation and flushing with O_2 -scrubbed Ar over the course of an hour. The anaerobic enzyme was then titrated with an anaerobic solution of $\sim 0.1 \text{ M}$ sodium dithionite in 50 mM HEPES, pH 7.2, monitoring enzyme reduction spectrophotometrically. The reduced enzyme was then mounted on the stopped-flow apparatus and mixed with varying concentrations of anaerobic, oxidized quinone substrate in 50 mM HEPES, pH 7.2, the reaction being monitored by the absorbance increase observed at 450 nm or 550 nm. Kinetic transients thus obtained were fit using the ProData Viewer package to obtain the rate constants, which were averaged and plotted as a function substrate concentration. When saturating kinetic behavior for k_{obs} as a function of [quinone] was observed, values for k_{ox} , the limiting rate constant at high [S], and dissociation constant, K_{d} , were obtained from hyperbolic fits to these plots using SigmaPlot (Systat Software, Inc.). When linear behavior was observed, the ratio $k_{\text{ox}}/K_{\text{d}}$ was determined directly from the slope.

Titration of CODH with quinones

Titration were performed using 4 μM or 8 μM CODH in 50 mM HEPES, pH 7.2 at 20°C. Titrations of oxidized enzyme with oxidized quinone were carried out aerobically, following the spectral change observed in the vicinity of 450 nm. Titration of oxidized enzyme with reduced quinone (prepared by directly bubbling Ar in a cuvette for 15 min to make anaerobic and titrated to reduction with 0.1 M sodium dithionite using a Hamilton syringe, following quinone reduction at 247 nm) was carried out anaerobically, by alternately evacuating and flushing the enzyme solution in an anaerobic cuvette with O_2 -scrubbed Ar gas for 1 hour. Aliquots of reduced 1,4-benzoquinone were then added with a Hamilton syringe and the spectral change in the visible monitored spectrophotometrically. For 1,4-

benzoquinone, plots of absorbance change vs. [quinone] were used to obtain K_d , which was determined by fitting the data to the hyperbolic equation:

$$A_{\text{obs}} = (\Delta A_{\text{max}} \cdot X) / (K_d + X)$$

Inhibition of CODH by diphenyliodonium chloride

Inactivation of the FAD cofactor of CODH was accomplished by covalent modification of the flavin with diphenyliodonium chloride using a modification of the procedure of Chakraborty and Massey (21). 10 μM CODH in 50 mM HEPES, pH 7.2 was flushed with Ar for 1 hr and reduced with ~2 fold excess sodium dithionite. Diphenyliodonium chloride was added to a final concentration of 1 mM and incubated at 20°C for 2 hr. Excess diphenyliodonium chloride was removed by G-25 column and the enzyme assayed for activity. Spectral changes and specific activity of the enzyme with ubiquinone-1 and methylene blue were used to assess the degree of inhibition, as described above.

Electron paramagnetic resonance spectroscopy

EPR spectra were recorded using a Bruker Instruments ER 300 spectrometer equipped with an ER 035M gaussmeter and HP 5352B microwave frequency counter. Temperature was controlled at 150 K using a Bruker ER 4111VT liquid N₂ cryostat. Samples were prepared by reducing 50 μM anaerobic CODH in 50 mM HEPES, pH 7.2 with a stock solution of 0.1 M dithionite, followed by addition of 0.5 equivalents of 1,4-benzoquinone or ubiquinone-1. Samples were immediately frozen in liquid N₂. Controls of 50 μM CODH in 50 mM HEPES, pH 7.2, either fully oxidized or fully reduced by titration with dithionite, were also prepared. A final sample of 50 μM CODH was prepared by first reducing the enzyme with 0.1 M dithionite and re-oxidizing with 12 equivalents of quinone prior to freezing.

RESULTS

CODH reactivity toward cytochrome *b*₅₆₁

Cytochrome *b*₅₆₁ was isolated from *O. carboxydovorans* as described in Materials and Methods and examined for reactivity toward CODH in both steady-state and rapid-reaction experiments. In the assays performed, cytochrome *b*₅₆₁ in 50 mM HEPES, pH 7.2, containing 0.2% Triton X-100 or N,N-dimethyldodecylamine-N-oxide was made anaerobic by repeated evacuation and flushing with O₂-scrubbed Ar followed by CO bubbling. The activity assay was carried out over 10 min observing total spectral change with an emphasis near 415 nm and 561 nm, but no reduction of cytochrome *b*₅₆₁ was seen in these experiments. Other cytochrome-containing fractions isolated from soluble and membrane cell fractions included multiple cytochromes *c*, and cytochrome *a*, and these were also examined for activity toward CODH; in no case was cytochrome reduction observed (supplemental figure 2). Only when 1,4-benzoquinone (at a concentration of 5 μM) was added to the assay with cytochrome *c* was reduction observed, as reflected in the absorbance increase at 550 nm and a shift of the Soret band from 410 nm to 415 nm. These results suggest that cytochrome reduction was mediated by the quinone, which served as the proximal oxidant for the enzyme.

Steady state kinetic studies

Based on the above results suggesting that 1,4-benzoquinone is an oxidizing substrate of CODH, a steady-state study was performed using 1,4-benzoquinone as oxidizing substrate. The assay was performed under the standard conditions of 25°C in 50 mM HEPES pH 7.2, with solutions of 8.4 μM to 191 μM 1,4-benzoquinone placed in a serum-stoppered cuvette

and bubbled first with argon and then CO to give a concentration of 400 μM . The reaction was followed by the spectral change at 246 nm associated with reduction of the quinone. Significant catalytic rates were observed. A plot of observed catalytic velocity versus [1,4-benzoquinone] was hyperbolic and a fit to the data yielded a k_{cat} of 104 s^{-1} , K_{m} of $16.4 \mu\text{M}$ and $k_{\text{cat}}/K_{\text{m}}$ of $6.37 \times 10^6 \text{ M}^{-1}\text{s}^{-1}$ (Supplementary Material, Figure 3). This is essentially identical to the previously observed k_{cat} of 93.3 s^{-1} using methylene blue as oxidizing substrate, consistent with the previous conclusion that the reductive half-reaction was principally rate-limiting (18). Ubiquinone-1 was also examined as substrate, but in this case it proved impossible to obtain sufficiently high concentrations of substrate to yield saturating kinetics given the limited water-solubility of ubiquinone-1. A plot of the observed catalytic velocity versus [ubiquinone-1] thus yielded a straight line, and from the slope a value for the ratio $k_{\text{cat}}/K_{\text{m}}$ of $5.81 \times 10^4 \text{ M}^{-1}\text{s}^{-1}$ was obtained. When the steady-state kinetics with ubiquinone-1 were repeated in D_2O , a solvent isotope effect of 1.4 was obtained from the ratio of $\text{H}(k_{\text{cat}}/K_{\text{m}})/\text{D}(k_{\text{cat}}/K_{\text{m}})$ (Supplementary Material, Figure 4).

With other enzymes of the XOR family, reducing equivalents enter at the molybdenum center in the reductive half of the catalytic sequence and leave via the FAD (after intramolecular electron transfer involving the iron-sulfur clusters) (1). In order to establish that quinone substrates interacted with CODH at its FAD site, the enzyme was reacted with diphenyliodonium chloride to covalently modify the FAD and render the cofactor redox-inert (21). Treatment of enzyme in this way lowered the steady state rates of ubiquinone-1 reduction by 83% and methylene blue by 80%; modification of the flavin was confirmed by comparing the absorption spectrum of the reoxidized, modified enzyme with that of the original (Figure 2). The unmodified minus modified difference spectra revealed features at 370 nm and 450 nm constant with flavin modification seen in xanthine oxidase (Figure 2, inset) (21). With the modified enzyme, reoxidation of the iron-sulfur clusters is observed after exposure to air, while the additional absorbance increase expected for reoxidation of the FAD is not observed. The reaction was carried out to longer time periods in order to achieve a greater degree of inhibition, but no further inhibition was observed. The incomplete inactivation was most likely due to incomplete covalent modification of the flavin due to the lower solvent accessibility of the FAD of CODH relative to xanthine oxidase. We observed, for example, that CODH inhibited with diphenyliodonium chloride regained slowly regained activity over time, suggesting that the inhibited flavin-diphenyliodonium chloride enzyme complex was slowly returned back to functional enzyme. Consistent with this, the absorbance of oxidized FAD is slowly recovered over the next 18 hr, reflecting the slow breakdown of the flavin-diphenyliodonium chloride complex to yield the oxidized cofactor (21).

Oxidative-Half Reaction of CODH with Quinone Substrates

The rapid reaction kinetics of the reoxidation of reduced CODH by several quinones was next examined by stopped-flow spectrophotometry at 25°C , following the reoxidation of enzyme at 450 nm. The substrates used were 1,4-benzoquinone, 1,4-naphthoquinone, 1,2-naphthoquinone-4-sulfonic acid and ubiquinone-1. Figure 3 shows a typical time course for the reaction with $25 \mu\text{M}$ 1,4-benzoquinone with $5 \mu\text{M}$ CODH after mixing in the stopped flow apparatus. At low substrate concentrations the reaction appeared biphasic with apparent rate constants of 37 s^{-1} for the first phase (with an associated absorbance change of 0.01 OD, 24% of the total absorbance change) and 3.33 s^{-1} for the second (with amplitude of 0.03 OD, 73% of the total absorbance change). (A third phase was sometimes observed at low substrate concentrations, with a rate constant 0.5 s^{-1} and absorbance change of $\sim 0.001 \text{ OD}$, 2% of the total absorbance change, that was attributed to oxygen contamination. This phase was neglected on the basis of the very small absorbance change associated with it.) The overall kinetic complexity of the reaction is a reflection of the fact that three equivalents of

quinone must react with the fully reduced enzyme in turn for full reoxidation. We attribute the first phase to the reaction of fully reduced (*i.e.*, six-electron-reduced) CODH with a first equivalent of 1,4-benzoquinone to yield four-electron reduced enzyme and 1,4-benzoquinone-H₂, and the second rate constant the subsequent reaction of four-electron reduced enzyme with two additional equivalents of 1,4-benzoquinone in turn (which are kinetically unresolved). At higher substrate concentrations, the amplitude of the faster process increases at the expense of the slower, the latter eventually disappearing by 500 μM . Plots of the observed rate constant versus [1,4-benzoquinone] were hyperbolic for both phases of the reaction; the first phase yielded a k_{ox} of 125.1 s^{-1} , K_{d} of $48 \text{ }\mu\text{M}$ and $k_{\text{ox}}/K_{\text{d}}$ (*i.e.*, the slope of the plot of k_{obs} versus [1,4 BQ]) of $2.60 \times 10^6 \text{ M}^{-1}\text{s}^{-1}$, while the second phase showed a k_{ox} of 32.7 s^{-1} and K_{d} of $154 \text{ }\mu\text{M}$. Again, the second phase was only clearly resolved below 500 μM 1,4-benzoquinone when 5 μM enzyme is used.

The reaction of reduced CODH with 1,2-naphthoquinone-4-sulfonic acid was also biphasic, with amplitudes of 0.02 OD (28% of the total observed spectral change) seen for the first phase and 0.04 OD (57% of the total spectral change) for the second when 5 μM CODH was used. A third very slow phase (0.01 OD, 14% of the total spectral change) was observed that was attributed to photosensitivity of the quinone, as confirmed by monitoring the spectral change of 1,2-naphthoquinone-4-sulfonic acid alone in the observation cell of the stopped-flow apparatus. This phase became negligible at substrate concentrations above 125 μM owing to the short time scale of the reaction. Due to the high extinction of 1,2-naphthoquinone-4-sulfonic acid, concentrations under 1 mM had to be used and it was not possible to reach saturating concentrations; only the ratio $k_{\text{ox}}/K_{\text{d}}$ could be obtained from the linear plot of k_{obs} versus [1,2-naphthoquinone-4-sulfonic acid], with values of $1.31 \times 10^5 \text{ M}^{-1}\text{s}^{-1}$ and $3.90 \times 10^4 \text{ M}^{-1}\text{s}^{-1}$ for the faster and slower phases, respectively.

1,4-naphthoquinone also exhibited biphasic behavior, with amplitudes of 0.04 OD (40% of the total observed spectral change) and 0.06 OD (60% of the observed spectral change) for the first and second phases, respectively, with 5 μM enzyme. 1,4-naphthoquinone (which is structurally similar to menaquinone) yielded somewhat slower kinetics than seen with 1,4-benzoquinone, with $k_{\text{ox}} = 38.1 \text{ s}^{-1}$, $K_{\text{d}} = 140 \text{ }\mu\text{M}$, and $k_{\text{ox}}/K_{\text{d}} = 2.72 \times 10^5 \text{ M}^{-1}\text{s}^{-1}$ for the faster phase of the reaction; the slower phase gave $k_{\text{ox}} = 6.0 \text{ s}^{-1}$, $K_{\text{d}} = 213 \text{ }\mu\text{M}$ and $k_{\text{ox}}/K_{\text{d}} = 2.82 \times 10^4 \text{ M}^{-1}\text{s}^{-1}$.

Ubiquinone-1 also showed biphasic behavior with amplitudes of 0.02 OD (14% of the total observed spectral change) and 0.12 (86% of the total spectral change) OD for the first and second phases, respectively, with 5 μM CODH. Due to the limited solubility of ubiquinone-1 it was again not possible to approach saturating conditions, and only a ratio $k_{\text{ox}}/K_{\text{d}}$ could be determined from the slope of the linear plot of k_{obs} versus [ubiquinone-1], with values of $2.88 \times 10^5 \text{ M}^{-1}\text{s}^{-1}$ and $1.99 \times 10^4 \text{ M}^{-1}\text{s}^{-1}$ obtained for the faster and slower phases, respectively. Plots of observed rate constant versus [quinone] for each substrate is shown in Figure 4, with the kinetic parameters thus determined summarized in Table 1. For the purposes of comparison, attention was focused on the faster phases of the overall reaction which reflected the reaction of fully reduced enzyme with the first equivalent of quinone in the course of reoxidation and thus represented the intrinsic reactivity of the fully reduced flavin site with quinone. It was evident that of the three quinones examined, 1,4-benzoquinone (which is structurally similar to ubiquinone) was the most effective substrate having a $k_{\text{ox}}/K_{\text{d}}$ an order of magnitude higher than the other two.

Titration of CODH with oxidized and reduced quinone

In order to establish the affinity of CODH for 1,4-benzoquinone, titrations of CODH with oxidized and reduced 1,4-benzoquinone were carried out. Figure 5 shows the titration of oxidized 1,4-benzoquinone with 8 μM CODH, with the greatest spectral change seen at 424

nm. The inset to Figure 5 inset shows a plot of the change in absorbance at 424 nm vs. [1,4-benzoquinone] from which a K_d of 100 μM can be determined. A comparison with the kinetically determined K_d for binding of oxidized 1,4-benzoquinone with reduced CODH of 48 μM indicates that oxidation of the enzyme flavin reduces affinity for the quinone by a factor of two. Titration of oxidized CODH with pre-reduced 1,4-benzoquinone under anaerobic conditions yielded an oxidized minus-reduced difference spectrum indicating that the FAD and Fe/S centers became fully reduced, as reflected by bleaching at 450 nm and 550 nm (Supplementary Material, Figure 5).

DISCUSSION

Here we have examined the reaction of reduced CODH with several cytochromes and quinones in an effort to determine the oxidizing substrate for the enzyme. Having failed in an exhaustive effort to identify a cytochrome capable of being effectively reduced by CODH, we find that several quinones are very effective substrates, rapidly oxidizing reduced CODH under anaerobic conditions. 1,4-benzoquinone is found to be the most effective oxidizing substrate, with a k_{ox} of 125.1 s^{-1} at pH 7.2, 25°C for the fastest phase of enzyme reoxidation. The multiple phases observed in the oxidative half-reaction kinetics seen here are attributed to the necessarily sequential nature of the reaction of fully (six-electron) reduced enzyme with three successive equivalents of quinone.

Although 1,4-benzoquinone was the most effective (and also most soluble) of the quinones tested, ubiquinone-1 was also a fairly effective substrate, but due to its low solubility in water only k_{ox}/K_d , $2.88 \times 10^5 \text{ M}^{-1}\text{s}^{-1}$ and k_{cat}/K_m , $5.81 \times 10^4 \text{ M}^{-1}\text{s}^{-1}$ could be determined experimentally – these were approximately an order of magnitude slower than seen with 1,4-benzoquinone, k_{ox}/K_d , $2.60 \times 10^6 \text{ M}^{-1}\text{s}^{-1}$. A similar situation has been seen in chromate reductase, a soluble quinone-reducing protein that best utilizes 1,4-benzoquinone over ubiquinone-1 (23). Both 1,4-naphthoquinone and 1,2 naphthoquinone-4-sulfonate were poorer oxidizing substrates for CODH, suggesting that the structurally related menaquinone is a less likely physiological substrate for the enzyme than ubiquinone. No semiquinone EPR signal was observed in EPR experiments monitoring catalytic enzyme turnover, and it appears that the principal oxidizing event is an effective two-electron process (supplemental figure 6). Finally, given the overall effectiveness of quinones as substrate, we conclude that one or another component of the quinone pool of *O. carboxidovorans* constitutes the proximal oxidizing substrate for CODH, and that cytochromes become reduced only subsequent to the introduction of reducing equivalents into the quinone pool.

Supplementary Material

Refer to Web version on PubMed Central for supplementary material.

References

1. Hille R. The Mononuclear Molybdenum Enzymes. Chem Rev. 1996; 96:2757–2816. [PubMed: 11848841]
2. Meyer O, Schlegel HG. Oxidation of Carbon Monoxide in Cell Extracts of *Pseudomonas carboxydovorans*. Arch Microbiol. 1978; 118:35–43. [PubMed: 697501]
3. Meyer O, Schlegel HG. Carbon Monoxide:Methylene Blue Oxidoreductase from *Pseudomonas carboxydovorans*. Bacteriol. 1980; 141:78–80.
4. Dobbek H, Gremer L, Meyer O, Huber R. Crystal structure and mechanism of CO dehydrogenase, a molybdo iron-sulfur flavoprotein containing S-selanyl cysteine. Proc Natl Acad Sci USA. 1999; 96:8884–8888. [PubMed: 10430865]

5. Dobbek H, Gremer L, Kiefersauer R, Huber R, Meyer O. Catalysis at a dinuclear [CuSMo(AO)OH] cluster in a CO dehydrogenase resolved at 1.1-Å resolution. *Proc Natl Acad Sci USA*. 2002; 99:15971–15976. [PubMed: 12475995]
6. Hänzelmann P, Dobbek H, Gremer L, Huber R, Meyer O. The Effect of Intracellular Molybdenum in *Hydrogenophaga pseudoflava* on the Crystallographic Structure of the Seleno-Molybdo-Iron-Sulfur Flavoenzyme Carbon Monoxide Dehydrogenase. *J Mol Biol*. 2000; 301:1221–1235. [PubMed: 10966817]
7. Gremer L, Kellner S, Dobbek H, Huber R, Meyer O. Binding of Flavin Adenine Dinucleotide to Molybdenum-containing Carbon Monoxide Dehydrogenase from *Oligotropha carboxidovorans*. *J Biol Chem*. 2000; 275:1864–1872. [PubMed: 10636886]
8. Kang BS, Kim YM. Cloning and Molecular Characterization of the Genes for Carbon Monoxide Dehydrogenase and Localization of Molybdopterin, Flavin Adenine Dinucleotide, and Iron-Sulfur Centers in the Enzyme of *Hydrogenophaga pseudoflava*. *J Bacteriol*. 1999; 181:5581–5590. [PubMed: 10482497]
9. Schübel U, Kraut M, Morsdorf G, Meyer O. Molecular characterization of the gene cluster *coxMSL* encoding the molybdenum-containing carbon monoxide dehydrogenase of *Oligotropha carboxidovorans*. *J Bacteriol*. 1995; 177:2197–2203. [PubMed: 7721710]
10. Santiago B, Schübel U, Egelseer C, Meyer O. Sequence analysis, characterization and CO-specific transcription of the *cox* gene cluster on the megaplasmid pHCG3 of *Oligotropha carboxidovorans*. *Gene*. 1999; 236:115–124. [PubMed: 10433972]
11. Gnida M, Ferner R, Gremer L, Meyer O, Meyer-Klaucke W. A Novel Binuclear [CuSMo] Cluster at the Active Site of Carbon Monoxide Dehydrogenase: Characterization by X-ray Absorption Spectroscopy. *Biochemistry*. 2003; 42:222–230. [PubMed: 12515558]
12. Ragsdale SW, Pierce E. Acetogenesis and the Wood-Ljungdahl pathway of CO₂ fixation. *Biochim Biophys Acta*. 2008; 1784:1873–1898. [PubMed: 18801467]
13. Cypionka H, Meyer O. Carbon Monoxide-Insensitive Respiratory Chain of *Pseudomonas carboxydovorans*. *J Bacteriol*. 1983; 141:74–80.
14. Meyer O, Gremer L, Ferner R, Ferner M, Dobbek H, Gnida M, Meyer-Klaucke W, Huber R. The role of Se, Mo and Fe in the structure and function of carbon monoxide dehydrogenase. *Biol Chem*. 2000; 381:865–876. [PubMed: 11076018]
15. Moersdorf G, Frunzke K, Gadkari D, Meyer O. Microbial growth on carbon monoxide. *Biodegradation*. 1992; 3:61–82.
16. Kim YM, Hegeman GD. Electron Transport System of an Aerobic Carbon Monoxide-Oxidizing Bacterium. *J Bacteriol*. 1981; 148:991–994. [PubMed: 6273386]
17. Meyer O, Schlegel HG. Reisolation of the carbon monoxide utilizing hydrogen bacterium *Pseudomonas carboxydovorans* (Kistner) comb. nov. *Arch, Microbiol*. 1978; 118:35–43. [PubMed: 697501]
18. Zhang B, Hermann C, Hille R. Kinetic and Spectroscopic Studies of the Molybdenum-Copper CO Dehydrogenase from *Oligotropha carboxidovorans*. *J Biol Chem*. 2010; 285:12571–12578. [PubMed: 20178978]
19. Resch, Dobbek H.; Meyer, O. Structural and functional reconstruction in situ of the [CuSMoO₂] active site of carbon monoxide dehydrogenase from the carbon monoxide oxidizing eubacterium *Oligotropha carboxidovorans*. *J Biol Inorg Chem*. 2005; 10:518–528. [PubMed: 16091936]
20. Albarran G, Schuler RH. Determination of the spectroscopic properties and chromatographic sensitivities of substituted quinones by hexachlorate(IV) oxidation of hydroquinone. *Talanta*. 2008; 74:844–850. [PubMed: 18371718]
21. Chakraborty S, Massey V. Reaction of Reduced Flavins and Flavoproteins with Diphenyliodonium Chloride. *J Biol Chem*. 2002; 277:41507–41516. [PubMed: 12186866]
22. Kita K, Vibat CRT, Meinhardt S, Guest JR, Gennis RB. One-step Purification from *Escherichia coli* of Complex II (Succinate:Ubiquinone Oxidoreductase) Associated with Succinate-reducible Cytochrome *b556*. *J Biol Chem*. 1989; 264:2672–2677. [PubMed: 2644269]
24. Gonzalez, Claudio F.; Ackerley, David F.; Lynch, Susan V.; Matin, A. ChrR, a Soluble Quinone Reductase of *Pseudomonas putida* That Defends against H₂O₂. *J Biol Chem*. 2005; 280:22590–22595. [PubMed: 15840577]

ABBREVIATIONS USED

CODH	CO dehydrogenase
HEPES	(4-(2-hydroxyethyl)-1-piperazineethanesulfonic acid)
XOR	xanthine oxidoreductase

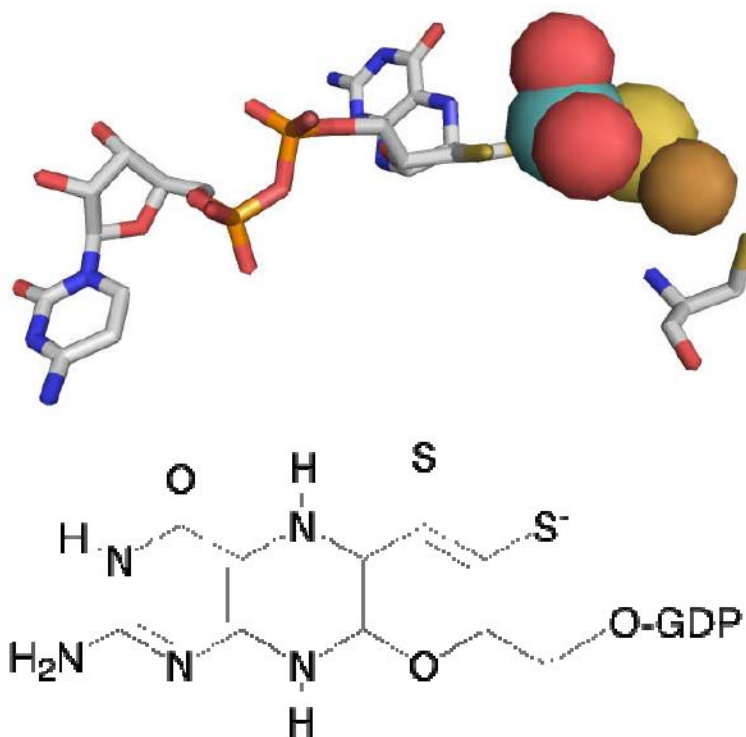


Figure 1. The active site of CODH

Top, the active site of the enzyme as rendered using PDB file 1N5W. Atom colors are CPK, with the molybdenum atom rendered in teal and the copper in copper color. Cys 388, which coordinates the copper, is shown at far right. *Bottom*, the structure of the pyranopterin cofactor of the binuclear center, which is present as the dinucleotide of guanine.

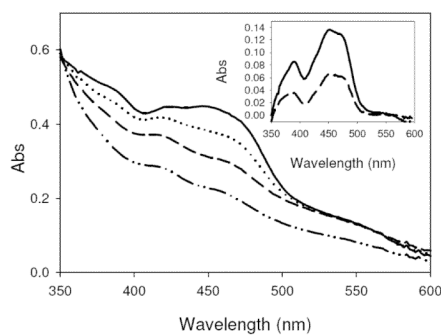


Figure 2. Diphenyliodonium chloride inhibition of CODH

A, The spectral change over the course of inhibition of CODH in 50 mM HEPES, pH 7.2, with diphenyliodonium chloride. Spectra are for oxidized CODH (—), dithionite-reduced CODH (- · · -), air oxidized CODH following diphenyliodonium chloride inhibition (- -), and diphenyliodonium chloride-inhibited CODH after 18hrs (····). *Inset*, The oxidized-minus-inhibited difference spectrum following diphenyliodonium chloride inhibition (—) and after an 18 hr incubation (- -).

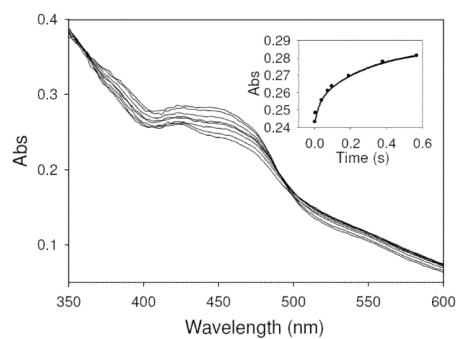
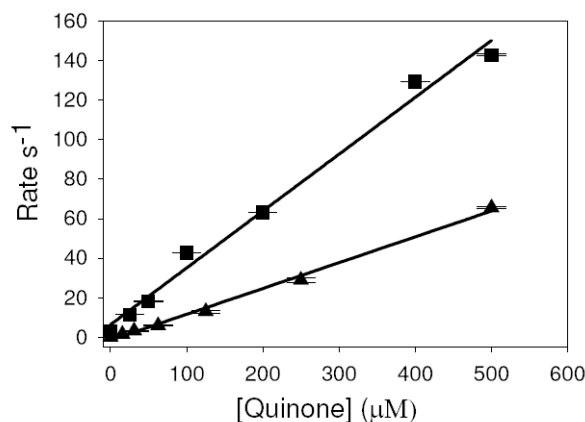


Figure 3. Oxidation of reduced CODH by 25 μ M 1,4-benzoquinone

Oxidation of dithionite-reduced 5 μ M CODH by 1,4-benzoquinone in 50 μ M HEPES, pH 7.2 25 $^{\circ}$ C, over 0.6 s. The traces shown are those recorded at 0.004 s, 0.007 s, 0.015 s, 0.027 s, 0.042 s, 0.076 s, 0.098 s, 0.0193 s, 0.0382 s and 0.0571 s increasing in absorbance from 0.004 s to 0.0571 s at 450 nm. *Inset*, Time course of absorbance change at 450 nm over 0.6 s (absorbance measurements shown are for 0.004 s, 0.007 s, 0.015 s, 0.027 s, 0.042 s, 0.076 s, 0.098 s, 0.0193 s, 0.0382 s and 0.0571 s) during the course of CODH oxidation. Fits to the data yield observed rate constants of 37 s $^{-1}$ for the first phase and 3.3 s $^{-1}$ for the second phase (with an R 2 value for the fit of 0.993).

A:



B:

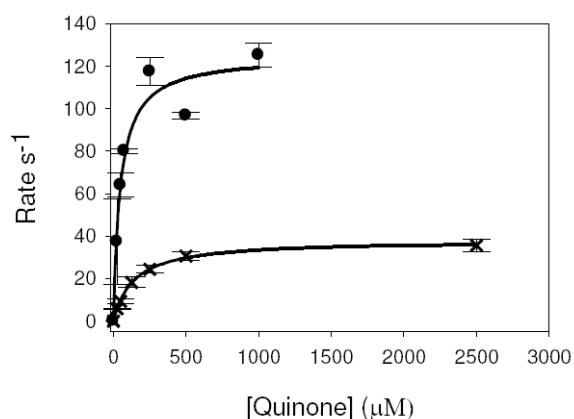


Figure 4. Substrate concentration dependence of reoxidation of dithionite-reduced CODH by quinones

A, plots of k_{fast} versus [quinone] for the reaction of 5 μM enzyme with ubiquinone-1 (■) and 1,2-naphthoquinone-4-sulfonic acid (▲) in 50 mM HEPES, pH 7.2, 25°C. Solid Line, fit with a linear equation using SigmaPlot (Systat Software, Inc.). The ratio $k_{\text{ox}}/K_{\text{d}}$ (corresponding to the second-order reaction of reduced enzyme with substrate in the low-[Q] regime) was determined by the slope of the fitted line, which for ubiquinone-1 and 1,2-naphthoquinone-4-sulfonic acid were $2.88 \times 10^5 \text{ M}^{-1} \text{ s}^{-1}$ ($R^2=0.990$) and $1.31 \times 10^5 \text{ M}^{-1} \text{ s}^{-1}$ ($R^2=0.995$), respectively. B, plots of k_{fast} versus [quinone] for the reaction of 5 μM enzyme with 1,4-benzoquinone (●) and 1,4-naphthoquinone (x) in 50 mM HEPES, pH 7.2, 25°C. Solid line, fit using the hyperbolic equation $k_{\text{obs}} = k_{\text{ox}}[Q]/(K_{\text{d}} + [Q])$ using SigmaPlot, where k_{ox} is the limiting rate constant for reoxidation at high [Q] and K_{d} is the dissociation constant for substrate binding. Kinetic parameters thus determined for 1,4-benzoquinone are k_{ox} , 125.1 s^{-1} , K_{d} , 46.7 μM , $k_{\text{ox}}/K_{\text{d}}$, $2.60 \times 10^6 \text{ M}^{-1} \text{ s}^{-1}$ (line fit $R^2= 0.955$) and for 1,4-

naphthoquinone are k_{ox} , 38.1 s^{-1} , K_d , $140 \text{ }\mu\text{M}$, and k_{ox}/K_d of $2.72 \times 10^5 \text{ M}^{-1} \text{ s}^{-1}$ (line fit $R^2 = 0.999$).

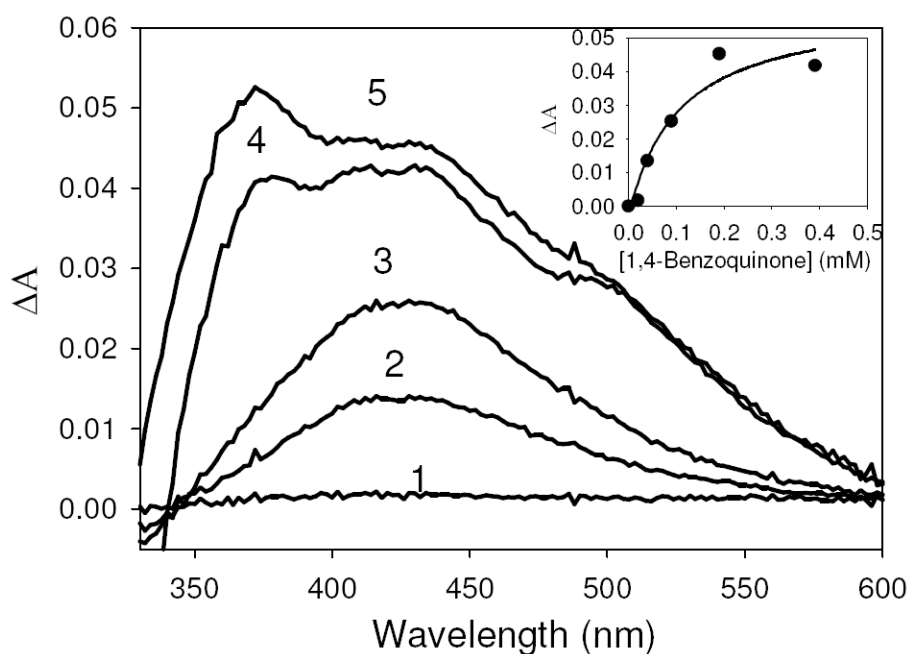


Figure 5. Titration of oxidized CODH with oxidized 1,4-benzoquinone
 Difference spectra of CODH with bound 1,4-benzoquinone in 50 mM HEPES, pH 7.2, minus oxidized CODH when CODH is titrated with oxidized 1,4-benzoquinone. Additions of 1,4 benzoquinone yielded final concentrations of 20 μM (1), 40 μM (2), 90 μM (3), 190 μM (4), 390 μM (5). *Inset*, concentration dependence of the spectral change at 424 nm produced by 1,4-benzoquinone titration with CODH. K_d was found to be 104 μM , determined by a fit using the hyperbolic equation $A_{\text{obs}} = (\Delta A_{\text{max}} \cdot x) / (K_d + x)$ ($R^2 = 0.9359$).

Table 1

Kinetic parameters of CODH oxidation by various quinones.

	K_d (μM)	k_{ox} (s^{-1})	k_{ox}/K_d ($\text{M}^{-1}\text{s}^{-1}$)	R^2 value for oxidative half fit data	K_m (μM)	k_{cat} (s^{-1})	k_{cat}/K_m ($\text{M}^{-1}\text{s}^{-1}$)	R^2 value for steady state fit data	KIE
1,4-benzoquinone	47.6	125.1	2.60×10^6	0.955	16.4	104.5	6.37×10^6	0.995	
1,4-naphthoquinone	140	38.1	2.72×10^5	0.999					
1,2-naphthoquinone-4-sulfonic acid			1.31×10^5	0.995					
Ubiquinone-1 H2O			2.88×10^5	0.990			5.81×10^4	0.980	1.41
Ubiquinone-1 D2O							4.13×10^4	0.996	